A Novel Strut-type Modular Robotic Structure using Rigid Node

Weibing Li, Robert C. Richardson and Jongrae Kim
School of Mechanical Engineering, University of Leeds, LS2 9JT, Leeds, U.K.

Keywords: Modular Robots, Rigid Nodes, Central Pattern Generators, Distributed Control, Physics-based Simulation.

Abstract: This paper proposes a novel way of constructing strut-type modular robotic structures to avoid some difficulties of designing and implementing ideal compliant nodes. Rigid nodes are employed to replace the ideal compliant nodes and to reduce the structural complexity while the feasibility of hardware implementation is dramatically improved. To release some kinematic constraints caused by the rigid nodes, we introduce robotic struts that consist of two prismatic actuators linked by a passive revolute joint. Physics-based robot models are constructed using a robot simulator. A scalable distributed control method is implemented using coupled central pattern generators. And, for comparison, the same control method is applied to conventional and the proposed strut-type modular robotic structures. Simulation results show that the proposed strut-type structures have several advantages over the conventional ones including less number of passive joints and shape-maintenance property.

1 INTRODUCTION

A modular robotic structure (MRS) consists of separate identical or different modules that can attach to or detach from each other to make the whole robot achieve manual or self-adaptive reconfiguration (Yim et al., 2007). One outstanding characteristic of MRSs is their shape-changing capability. In modular robotics, the following two shape-changing methods have been widely studied:

- Reconfiguration: an MRS can change its configuration (i.e., connectivity) by attaching and detaching robotic modules manually or self-adaptively.
- Deformation: an MRS with a specific configuration can change its shape without changing the connectivity of robotic modules.

Reconfiguration endows an MRS with a wide range of robotic structures which can emulate conventional monolithic robots and are suitable for different tasks under different working environments. Being different from reconfiguration, deformation can be used to adjust the MRS shape to internal and external forces exerted on the robotic structure.

To utilize the benefits generated from reconfiguration and deformation, numerous MRSs have been designed and developed. Most of the existing MRSs have block-like modules fitted with only revolute actuators (Zhang et al., 2003; Kurokawa et al., 2006; Østergaard et al., 2006; Salemi et al., 2006; Yim et al., 2007; Spröwitz et al., 2014), which are suitable for reconfiguration. Relatively less attention is given on strut-type MRSs using prismatic actuators (Curtis et al., 2007; Lyder, 2010; Yu, 2010; Zagal et al., 2012), which are adept at deformation. A design case of using both prismatic and revolute actuators can be found in (Baca et al., 2014). Usually, a revolute actuator can only rotate around its axis, while a prismatic actuator can elongate its body to reach some positions in the workspace directly. Prismatic actuators can form parallel truss-based structures that provides inherent stability. Hence, prismatic actuators may be more suitable for industrial activities such as load transportation than revolute actuators (Ramchurn et al., 2006).

In recent years, researchers have designed different strut-type MRSs using prismatic actuators for investigating their deformation and locomotion capabilities. Ideally, a strut-type MRS should have an ideal node connector mechanism which can connect numerous robotic struts. More importantly, robotic struts can rotate around the node center with some passive three degrees-of-freedom spherical joints and robotic struts connected by a same node should have a common center of rotation. In most simulations of the existing literature, robotic struts are jointed by point-like ideal nodes. Such point-like ideal nodes is helpful to reducing the complexity of kinematics (Hamlin and Sanderson, 1998) and providing compliant capability for strut-type MRSs, however, physical implementa-

Li, W., Richardson, R. and Kim, J.
A Novel Strut-type Modular Robotic Structure using Rigid Node.
DOI: 10.5220/0006004502610268
In *Proceedings of the 13th International Conference on Informatics in Control, Automation and Robotics (ICINCO 2016) - Volume 1*, pages 261-268
ISBN: 978-989-758-198-4

tion of such ideal nodes is highly difficult and even impossible (Lyder, 2010).

A lot of efforts have been made to design and implement an ideal compliant node. In the Tetrobot project (Hamlin and Sanderson, 1998), a centric multilink spherical (CMS) joint mechanism was designed, which can let the extended lines of its connected struts intersect at a same point. Such a CMS joint design can not only make a homogeneous design of Tetrobot possible but also simplify the kinematics of structures. However, CMS joint cannot be used to form chain-type structures. Additionally, CMS joints tend to become too weak to sustain a massive robotic structure. Moreover, the Tetrobot is hard to reconfigure as adding or removing struts usually need to disassemble the whole robotic structure (Lyder, 2010).

A workaround for constructing strut-type MRSs is to use struts that have their own center of rotation on the node surface. In such a solution, ball-and-socket joints and universal joints are commonly employed. In (Yu, 2010; Lyder, 2010), passive ball-and-socket joint based designs were adopted to provide compliant movements. Another well-known connector mechanism is the one designed by NASA for a 12-tetrahedron (12-TET) robot (Curtis et al., 2007). Specifically, NASA researchers developed two types of connectors, one is a wheel-shaped node for locomotion and the other one is a special payload node. The nodes endow itself with compliant flexibility by using passive universal joints. It is worth pointing out that the above non-ideal compliant nodes do simplify the physical implementation but make the kinematic analysis more complex (Lyder, 2010). This may be the reason why prototypes (e.g., Odin and 12-TET modular robots) using such compliant nodes are difficult to control and can only complete simple locomotion and/or deformation tasks.

Apart from the node design, another challenge in modular robotics is to construct a unified control framework that is both suitable to different modular robotic systems and scalable to robot size. Due to the modularity of modular robots, distributed control methods are intrinsically more scalable than centralized control methods. The scalability of a phase-automata based distributed control method developed for chain-type PolyBot modular robots has been validated by using a physical snake robot with 55 modules (Zhang et al., 2003). In (Yu, 2010), a scalable control framework for realizing coordinating locomotion of amorphous MRSs was established, analyzed and verified. Such a scalable control framework is based on a central pattern generator (CPG) based distributed control method.

Based on the above understanding, we focus on using rigid nodes for constructing strut-type MRSs to avoid the difficulty of implementing ideal compliant nodes. Unlike passive compliant nodes, struts connected using rigid nodes can not rotate passively around the nodes. Rather, by connecting struts rigidly using rigid nodes, the extended lines of struts intersect at a same point, which simplifies the kinematics complexity. To release some kinematic constraints caused by using rigid nodes, we use robotic struts that are comprised of two prismatic actuators linked by a passive revolute joint. For validating the proposed way of constructing strut-type MRSs, a scalable distributed control method is developed inspired by (Yu, 2010).

This paper is organized as follows: firstly, a novel strut-type modular robotic structure is presented; secondly, a control method using central pattern generator is designed based on a moving principle of which the performance is demonstrated by a prototype; thirdly, locomotion and deformation capabilities are verified by simulations; and finally, conclusions are presented.

2 ROBOTIC STRUCTURE & CONTROL

In this section, a novel strut-type MRS is to be introduced and details about the robot modeling and controller development environments including a CPG control method are to be presented.

2.1 Strut-type MRSs

Two strut-type MRSs are illustrated: one is conventional MRSs using ideal nodes and the other one is the proposed MRSs using rigid nodes. Figure 1(a) shows a conventional square-shaped MRS of which each strut has two prismatic actuators. The four robotic struts are connected using ideal compliant nodes equipped with passive revolute joints. Hence, the struts jointed by the same node can rotate around a common center of rotation. Each revolute joint has a rotation range of 80 degrees (Yu, 2010). As mentioned before, such ideal nodes are very difficult to design and implement. To avoid this implementation difficulty and reduce the kinematics complexity, rigid nodes are proposed for connecting robotic struts as shown in Figure 1(b).

Besides, differing from conventional struts that only have prismatic actuators, each strut is comprised of two prismatic actuators and one revolute actuator. To release the kinematic constraints introduced by rigid nodes, we let the revolute actuator be passive to add compliance for MRSs. To the authors' best

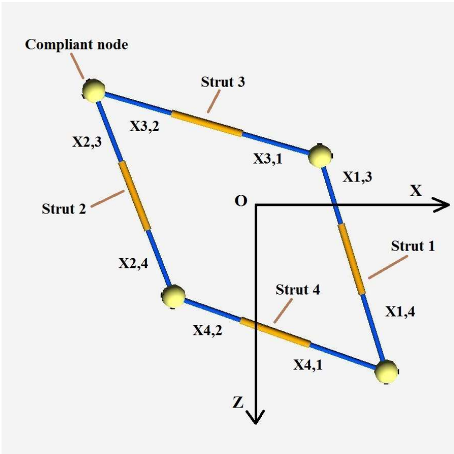

(a) A square robot with ideal compliant nodes.

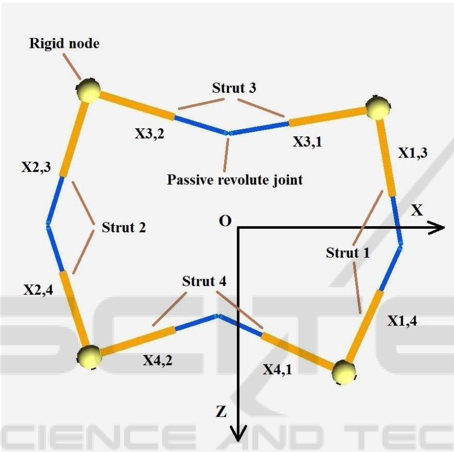

(b) A square robot with rigid nodes.

Figure 1: Square robots with compliant and rigid nodes.

knowledge, such a hybrid strut design has never been investigated and reported in the literature. Considering the type of actuators and joints used within each strut of the square robots, for convenience, hereafter, we term the robots shown in Figure 1(a) and (b) as RPPR (with R and P separately representing revolute and prismatic actuators) and PRP square robots, respectively. For constructing more complex structures, we consider each square robot as a meta-module, then arbitrary robotic structures can be constructed by rigidly connecting such square meta-modules.

To obtain movements of a robotic strut, one can let the two connected nodes work alternatively as a fixed anchor resorting to a friction-changing mechanism on the node bottom (Cheng et al., 2010). In this paper, to prevent from designing a friction-changing mechanism, we use the following moving steps to achieve a worm-like locomotion of a robotic strut with two prismatic actuators (Yu, 2010):

- Step 1: extend one of the prismatic actuators and keep the other one still;
- Step 2: retract the fully extended prismatic actuator and extend the other one simultaneously;
- Step 3: retract the fully extended prismatic actuator and keep the other one still.

For better understanding, we have tested such a moving principle using a physical strut controlled by an Arduino Uno board. Figure 2 shows the experimental test results. Initially, the prismatic actuators are fully retracted. Then, following the above moving steps periodically, the robotic strut can obtain a worm-like locomotion due to the change of its mass center during the task execution process.

Remarks. As illustrated in Figure 3, initially, the robotic strut keeps still and the normal forces N_1 and N_2 as well as the gravity force G should satisfy $N_1 + N_2 = G$ and $N_1 = N_2 = G/2$. During Step 1, when actuating the left prismatic actuator, at the first few seconds, friction forces $f_1 = \mu N_1$ (with μ denoting the friction coefficient) and $f_2 = \mu N_2$ would less than the actuation force F. Hence, Node 2 would move rightward for a short time while Node 1 will move leftward. Since the mass center of the whole strut moves leftward and $N_1 + N_2 = G$ together with $G \times l_1 = N_1 \times l_2$, N_2 and f_2 increases while N_1 and f_1 decreases. Therefore, Node 2 would keep still and Node 1 keeps moving leftward. During Step 2, due to the collective work of actuation forces F_1 and F_2, the horizontal resultant force exerted on the two nodes would be around 0 (we assume $F_1 = F_2$). Since such a force is less than the maximum static friction forces of the two nodes, the two nodes would not move. For the outer casing, owing to its resultant force $F_1 + F_2$, it will move leftward. The motion analysis of Step 3 is similar to Step 1, during Step 3, Node 2 would keep moving leftward while Node 1 would first keep still and then move rightward for a few seconds.

2.2 CPG Control Method

Inspired by (Yu, 2010) and (Sato et al., 2011), a CPG based distributed control method is implemented for comparing and investigating the conventional and proposed strut-type MRSs. Each square meta-module runs the developed identical controller. Initially, each CPG oscillator for each square robot has its own phase $\varphi(0)$. To achieve a coordinating movement of a whole structure comprised of several square meta-modules, the following control law is used to update the oscillator phase:

$$\varphi_i(k+1) = \varphi_i(k) + \gamma \sum_{j \in N_i} (\varphi_j(k) - \varphi_i(k) - \varphi_{ij}^*), \quad (1)$$

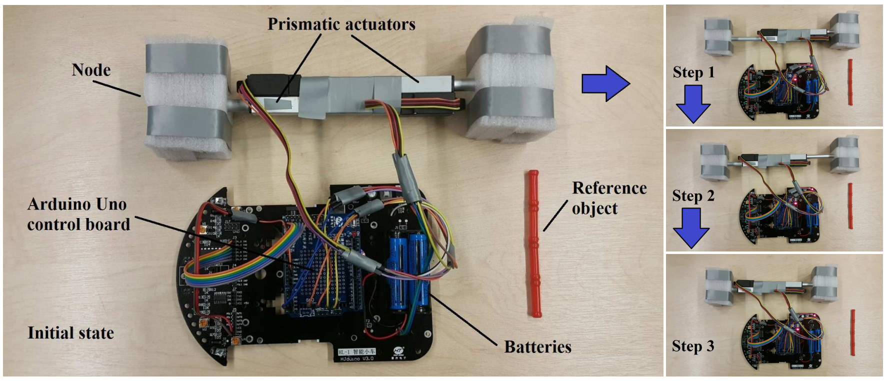

Figure 2: Experimental test of the employed moving principle within one cycle.

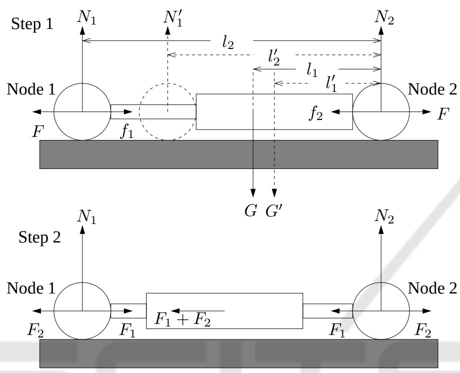

Figure 3: Force analysis of the employed moving principle.

where $\varphi_i(k)$ represents a part of the ith oscillator's phase at the kth time step, parameter γ is related to the convergence speed of (1), and N_i denotes a set containing square meta-module i's neighboring modules. Constant φ^*_{ij} is the desired phase offset between square meta-modules i and j. With respect to a moving direction, we have

$$\varphi^*_{ij} = \begin{cases} \pi, & \text{if } j \text{ is in front of } i \\ -\pi, & \text{if } j \text{ is at back of } i \\ 0, & \text{if } j \text{ is in parallel with } i \end{cases}$$

then, by considering intrinsic frequency of the CPG oscillator, we can have

$$\theta_i(k) = \omega k + \varphi_i(k), \tag{2}$$

where ω and $\theta_i(k)$ denote the oscillator frequency and oscillator phase, respectively.

For a square meta-module shown in Figure 1, we can have four cardinal traveling directions, i.e., a square robot can move along the positive and negative directions of X- or Z-axis. We use index 1, 2, 3, 4 for representing the traveling direction, which is listed in Table 1. Let d and d' denote the traveling and opposite directions, respectively. Set Ω represents the struts that can enable the square robot move along the traveling direction once they are actuated. By using the index schemes shown in Figure 1 and Table 1, for all $i \in \Omega$, we do the following computation:

$$\phi_{i,d}(k) = \mathrm{mod}(\theta_i(k), \frac{3\pi}{2}), \tag{3}$$

$$\phi_{i,d'}(k) = \mathrm{mod}(\theta_i(k) - \frac{\pi}{2}, \frac{3\pi}{2}). \tag{4}$$

In this way, the oscillator phase $\theta_i(k)$ is forced to become cyclic signals $\phi_{i,d}(k)$ and $\phi_{i,d'}(k)$ with a period of $3\pi/2$. Finally, the following activation function (AF) is exploited to obtain the corresponding set points $x_{i,d}(k)$ and $x_{i,d'}(k)$:

$$f(\phi) = \begin{cases} L\sin^2(\frac{\pi}{2}\sin^2(\frac{\pi}{2}\phi/P)), & \text{if } 0 < \phi < \pi \\ 0, & \text{otherwise} \end{cases} \tag{5}$$

where L indicates the fully extended length of a prismatic actuator and P is a constant parameter related to the period of the output signal. With respect to time, Figure 4 shows profiles of the designed AF (5) (i.e., AF I) and the AF presented in (Yu, 2010) (i.e., AF II). Note that the profile of (5) is smoother than that of AF II. Actually, AF II is not continuous, which may damage the physical motor as the motor velocity has to change abruptly at time 0s, 2.5s, 5s,10s,12.5s and 15s. Such a case can be avoided using the continuous function (5). One can easy to prove that the nth (with $n = 1,2,3\ldots$) order derivative of (5) would be 0 when $\phi = 0$ or $\phi = P$. Hence, the AF (5) is more suitable than AF II for motion planning in robotics. Besides,

Table 1: Index scheme for traveling directions.

Direction	Index
+X	1
-X	2
-Z	3
+Z	4

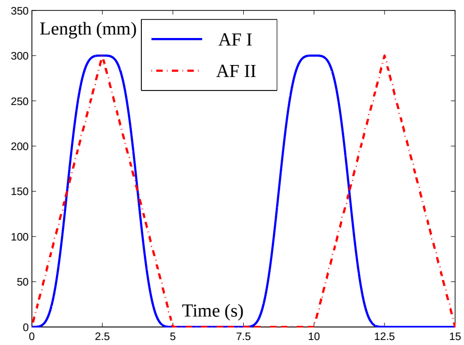

Figure 4: Two different activation functions.

AF (5) has a period of 7.5s (5s for actuation and 2.5 for keeping still) while AF II has a period of 10s (5s for actuation and 5s for keeping still). This is because we find it can speed up the locomotion process by decreasing the time for keeping still.

3 SIMULATIONS

To validate the performance of the proposed way of constructing strut type MRSs, simulations are conducted comparatively. Specifically, MSRs with one and two square meta-modules are investigated first. Then, we study the locomotion of an MSRs with six PRP square meta-modules. After that, a tentative deformation test is finally performed using an MSR with 37 PRP struts.

Inspired by some successful work (Spröwitz et al., 2014), Webots is used as the robot simulator. Webots is a physics-based simulator developed by Cyberbotics. By using a scene hierarchical tree, a robot model in Webots directly describes the geometric, kinematic and dynamic relationships of the robotic components as well as between the robotic system and its working environment.

3.1 Locomotion

This subsection investigates the locomotion capability of strut-type MRSs. We first study a single square meta-module, then MRSs with two and six square meta-modules are studied. Note that, for the comparative simulations, same initial phase values are employed for a relatively fair comparison.

3.1.1 Single Square Module

Figures 5 and 6 show an RPPR and a PRP square robots moving rightward (i.e., along the +X direction) using the mentioned moving principle. The conventional RPPR square robot can move faster than

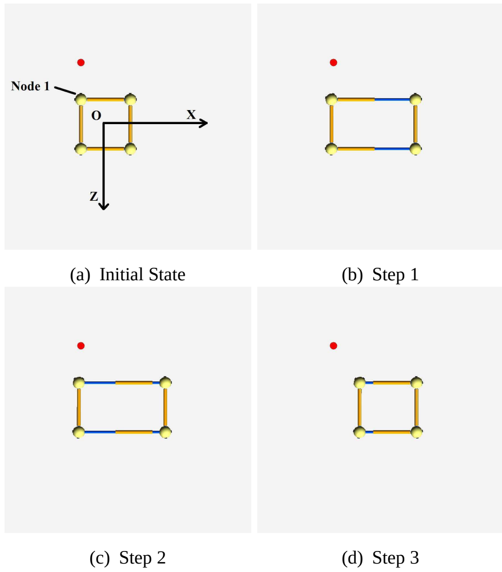

Figure 5: Conventional square robot obtain a worm-like locomotion within one cycle.

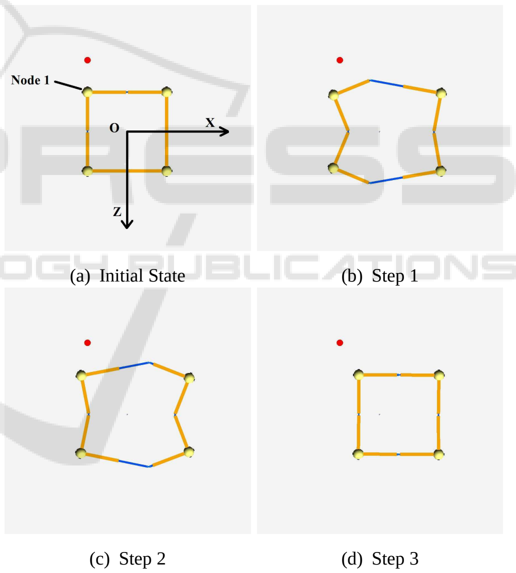

Figure 6: Proposed square robot obtain a worm-like locomotion within one cycle.

the proposed one, since the PRP square robot experiences deformations as shown in Figure 6(b) and (c). Such a fact can be seen in Figure 7 from which we can observe that, after actuating the square robots for 32s, the RPPR and PRP square robots move rightward around 1.0m and 0.7m, respectively.

3.1.2 Two Square Modules

In this part, we let MRSs with two square meta-modules move forward (i.e., along the -Z direction).

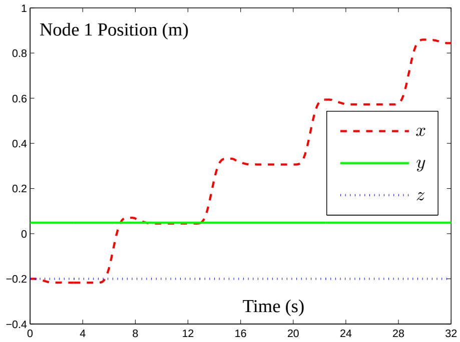

(a) Position profiles of the RPPR square robot

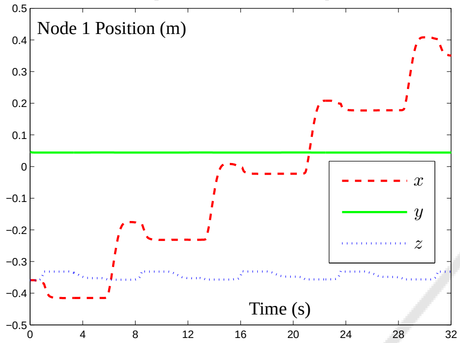

(b) Position profiles of the PRP square robot

Figure 7: Position profiles synthesized using CPG neural network based control method.

The corresponding results are shown in Figures 8 and 9. As seen from Figure 8(a)–(d) and Figure 9(a)–(d), initially, both the two kinds of MRSs can not move efficiently. After coordinating the phases between the two square meta-modules, a worm-like locomotion can be obtained as shown in Figure 8(e)–(h) and Figure 9(e)–(h). Even though the conventional MRS can still move slightly faster than the proposed MRS, it keeps an unstructured shape when achieving a coordinated locomotion. Unlike the conventional MRS, after some initial deformations, the proposed PRP MSR can restore and maintain its structured shape. This is important, as collisions between modules are more common when moving with an unstructured shape.

3.1.3 Six Square Modules

For further validation, we established MRSs with six square meta-modules. The corresponding simulation results are presented in Figure 10. From the figure, we can see that the MRSs can obtain a coordinating locomotion using the CPG control method. Specifically, oscillator phases are updated with desired phase offsets achieved and actuators' actual profiles finally coincide with their desired counterparts. Note that, during the task execution, square meta-module 0's prismatic actuators $x_{2,3}$ and $x_{2,4}$ are locked. Therefore,

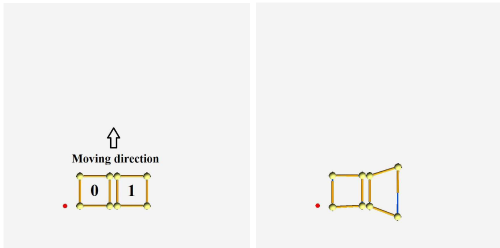

(a) Structure labels (b) Snapshot 1

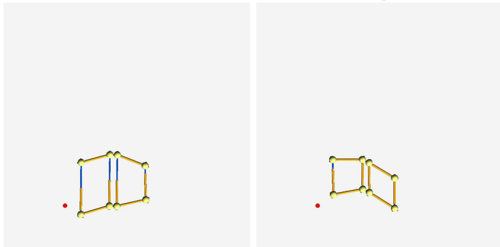

(c) Snapshot 2 (d) Snapshot 3

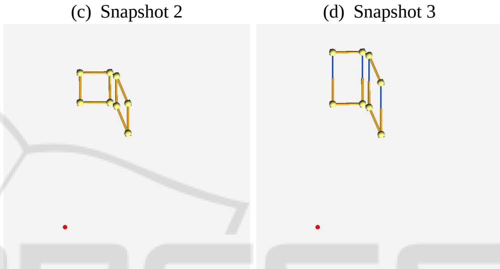

(e) Snapshot 4 (f) Snapshot 5

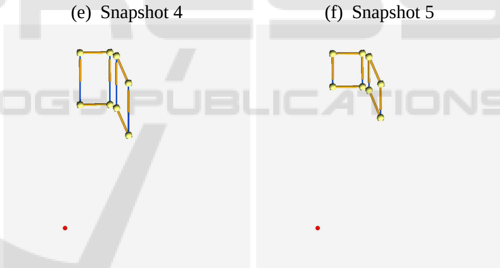

(g) Snapshot 6 (h) Snapshot 7

Figure 8: Locomotion of conventional MSR with two square meta-modules.

desired values for $x_{2,3}$ and $x_{2,4}$ are 0. For readability, we only show the first 60s profiles of actuated actuators $x_{4,1}$ and $x_{4,2}$ of square meta-module 0. The deviation in the $x_{4,1}$ profile may result from unexpected kinematic singularities. In future work, we will devote time to coping with this phenomenon.

3.2 Deformation

A simulation is performed to show the deformation capability of the proposed strut-type MRSs. Specifically, we construct an MRS with 37 PRP struts as shown in Figure 11(a). By actuating PRP struts placed along the top and bottom segments of the

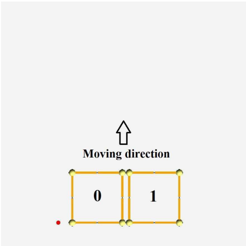

(a) Structure labels

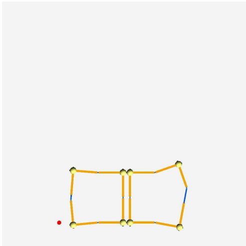

(b) Snapshot 1

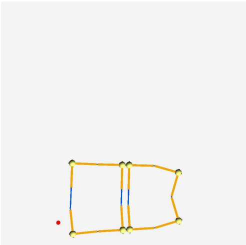

(c) Snapshot 2

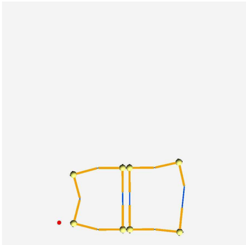

(d) Snapshot 3

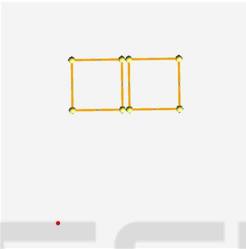

(e) Snapshot 4

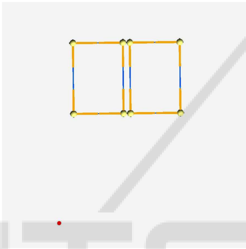

(f) Snapshot 5

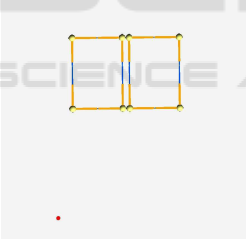

(g) Snapshot 6

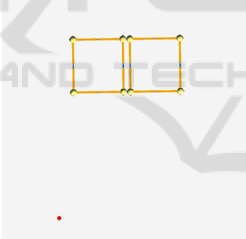

(h) Snapshot 7

Figure 9: Locomotion of proposed MSR with two square meta-modules.

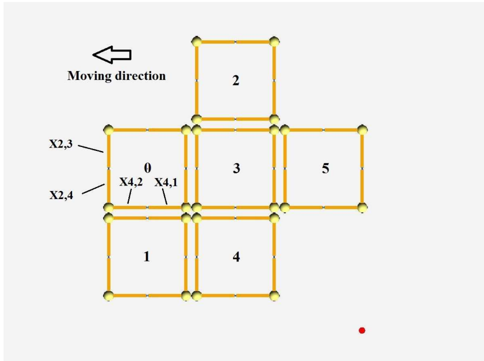

(a) Structure labels

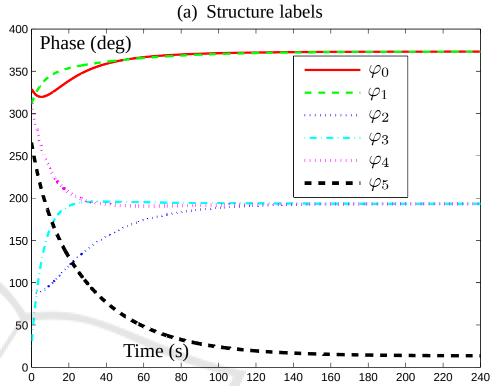

(b) Phase profile

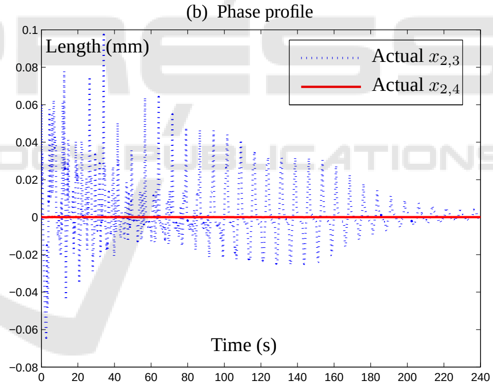

(c) $x_{2,3}$ and $x_{2,4}$ profiles of square module 0 (with desired values being 0)

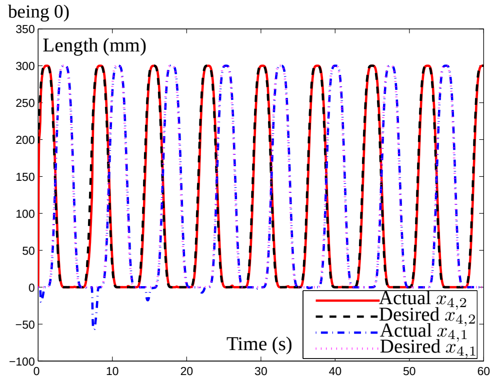

(d) $x_{4,2}$ and $x_{4,1}$ profiles of square module 0

Figure 10: Synthesized simulation results of an MSR with six square meta-modules.

perimeter using (2)–(5) (with $L = 50$mm and $\varphi_i(k) = 0$rad) and letting other struts be passive, we obtain the deformation result shown in Figure 11(b). Such a deformation can be used for physical display.

4 CONCLUSIONS

This paper presents a novel way of constructing strut-type MRSs using rigid nodes and robotic struts equipped with two prismatic and one revolute actuators. For testing such conceptual structures, Webots is used to construct the physics-based robot models.

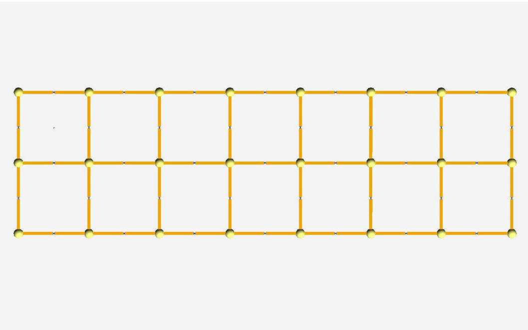

(a) Original shape

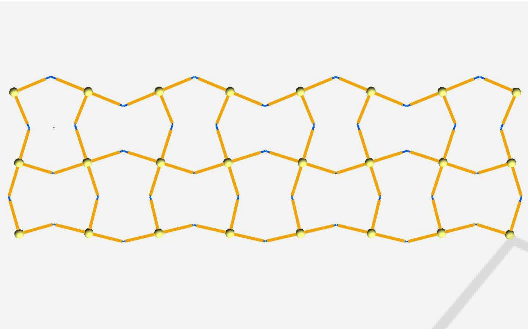

(b) Deformation shape

Figure 11: Deformation test of an MRS with 37 PRP struts.

Then, a CPG based control method is implemented for verifying the performance of the proposed MRSs. Comparative simulation results demonstrate the efficacy of the control method and the proposed MRSs as compared with conventional MRSs. Note that, by using rigid nodes, the difficulty of implementing ideal compliant nodes has been avoided, thus simplifying the mechanical design process. Future work will focus on investigating useful deformation of the MRSs, designing and building the proposed MRSs, and verifying the control method using physical MRSs.

REFERENCES

Baca, J., Hossain, S. G. M., Dasgupta, P., Nelson, C. A., and Dutta, A. (2014). ModRED: Hardware design and reconfiguration planning for a high dexterity modular self-reconfigurable robot for extra-terrestrial exploration. *Robotics and Autonomous Systems*, 62(7):1002–1015.

Cheng, N., Ishigami, G., Hawthorne, S., Chen, H., Hansen, M., Telleria, M., Playter, R., and Iagnemma, K. (2010). Design and analysis of a soft mobile robot composed of multiple thermally activated joints driven by a single actuator. In *Proceedings of the IEEE International Conference on Robotics and Automation*, pages 5207–5212.

Curtis, S., Brandt, M., Bowers, G., Brown, G., Cheung, C., Cooperider, C., Desch, M., Desch, N., Dorband, J., Gregory, K., Lee, K., Lunsford, A., Minetto, F., Truszkowski, W., Wesenberg, R., Vranish, J., Abrahantes, M., Clark, P., Capon, T., Weaker, M., Watson, R., Olivier, P., and Rilee, M. L. (2007). Tetrahedral robotics for space exploration. In *Proceedings of the IEEE Aerospace Conference*, pages 1–9.

Hamlin, G. J. and Sanderson, A. C. (1998). *TETROBOT: A Modular Approach to Reconfigurable Parallel Robotics*. Springer, New York.

Kurokawa, H., Yoshida, E., Tomita, K., Kamimura, A., Murata, S., and Kokaji, S. (2006). Self-reconfigurable M-TRAN structures and walker generation. *Robotics and Autonomous Systems*, 54(2):142–149.

Lyder, A. (2010). *Towards Versatile Robots Through Open Heterogeneous Modular Robots*. PhD thesis, University of Southern Denmark.

Østergaard, E. H., Kassow, K., Beck, R., and Lund, H. H. (2006). Design of the ATRON lattice-based self-reconfigurable robot. *Autonomous Robots*, 21(2):165–183.

Ramchurn, V., Richardson, R. C., and Nutter, P. (2006). ORTHO-BOT: A modular reconfigurable space robot concept. In Tokhi, M., Virk, G., and Hossain, M., editors, *Climbing and Walking Robots*, pages 659–666. Springer, Berlin Heidelberg.

Salemi, B., Moll, M., and Shen, W.-M. (2006). SUPERBOT: A deployable, multi-functional, and modular self-reconfigurable robotic system. In *Proceedings of the IEEE/RSJ International Conference on Intelligent Robots and Systems*, pages 3636–3641.

Sato, T., Kano, T., and Ishiguro, A. (2011). On the applicability of the decentralized control mechanism extracted from the true slime mold: a robotic case study with a serpentine robot. *Bioinspiration and Biomimetics*, 6(2):026006.

Spröwitz, A., Moeckel, R., Vespignani, M., Bonardi, S., and Ijspeert, A. J. (2014). Roombots: A hardware perspective on 3D self-reconfiguration and locomotion with a homogeneous modular robot. *Robotics and Autonomous Systems*, 62(7):1016–1033.

Yim, M., Shen, W.-M., Salemi, B., Rus, D., Moll, M., Lipson, H., Klavins, E., and Chirikjian, G. S. (2007). Modular self-reconfigurable robot systems [grand challenges of robotics]. *IEEE Robotics Automation Magazine*, 14(1):43–52.

Yu, C.-H. (2010). *Biologically-Inspired Control for Self-Adaptive Multiagent Systems*. PhD thesis, Harvard University.

Zagal, J. C., Armstrong, C., and Li, S. (2012). Deformable octahedron burrowing robot. In Adami, C., Bryson, D. M., Ofria, C., and Pennock, R. T., editors, *Artificial Life 13*, pages 431–438. MIT Press, Cambridge.

Zhang, Y., Yim, M., Eldershaw, C., Duff, D., and Roufas, K. (2003). Scalable and reconfigurable configurations and locomotion gaits for chain-type modular reconfigurable robots. In *Proceedings of the IEEE International Symposium on Computational Intelligence in Robotics and Automation*, pages 893–899.